

Synchronization of Coupled Oscillators: The Taylor Expansion of the Inverse Kuramoto Map

Elizabeth Y. Huang¹, Saber Jafarpour¹, Francesco Bullo¹

Abstract—Synchronization in the networks of coupled oscillators is a widely studied topic in different areas. It is well-known that synchronization occurs if the connectivity of the network dominates heterogeneity of the oscillators. Despite extensive study on this topic, the quest for sharp closed-form synchronization tests is still in vain. In this paper, we present an algorithm for finding the Taylor expansion of the inverse Kuramoto map. We show that this Taylor series can be used to obtain a hierarchy of increasingly accurate approximate tests with low computational complexity. These approximate tests are then used to estimate the threshold of synchronization as well as the position of the synchronization manifold of the network.

I. INTRODUCTION

Problem description and motivation: Synchronization is a ubiquitous phenomenon which appears naturally in various areas including physics, biology, and chemistry. One of the well-known models for studying synchronization of coupled oscillators is the Kuramoto model. Kuramoto model and its generalizations has been used for studying synchronization in various applications including pacemaker cells in heart [21], neural oscillators [6], deep brain simulation [27], spin glass models [16], oscillating neutrinos [23], chemical oscillators [17], multi-vehicle coordination [18], [25], synchronization of smart grids [11], security analysis of power flow equations [4], [30], optimal generation dispatch [19], and droop-controlled inverters in microgrids [7], [26].

Frequency synchronization is arguably one of the most important notions of synchronization for Kuramoto model. Frequency synchronization of Kuramoto coupled oscillators has been studied extensively in physics, dynamical system, and control communities. In the literature, many efficient numerical methods have been developed to study frequency synchronization of the Kuramoto model. However, for the purpose of analysis and design of networks of coupled oscillators, these numerical methods have several drawbacks. First, in many applications (such as power networks), the network contains many time-varying or unknown parameters (such as power injections/demands). Therefore any numerical study of synchronization requires implementing computations for a wide range of parameters, which is not computationally tractable for large networks. Secondly, these numerical methods usually do not provide any guarantee

for the performance of the synchronization such as robustness with respect to disturbances. Finally, these numerical methods do not provide any intuition about the role of different factors, such as network topology and dissimilarity of the oscillators, in the synchronization of Kuramoto model. Therefore they are not suited for design purposes. These observations motivate the quest for sharp analytic conditions for synchronization of Kuramoto model [2], [10], [5]. The first rigorous analytic characterization of frequency synchronization is developed for the complete unweighted graphs [3], [22], [28]. Further characterization of the frequency synchronization has been obtained for complete unweighted bipartite graphs [29]. Unfortunately these synchronization conditions require solving implicit algebraic equations and they are not suitable for studying the synchronization performance of the network. Moreover, they are only applicable to specific networks and cannot be extended for characterizing frequency synchronization of the Kuramoto model with general topologies. For the Kuramoto model with general topology and arbitrary weights, an ingenious approach based on graph theoretic ideas is proposed in [14]. Using this approach and Lyapunov analysis, a concise closed-form condition for synchronization of coupled oscillator is obtained [14]. Similar conditions have been derived in the literature using quadratic Lyapunov function [8], [9] and sinusoidal Lyapunov function [12]. The essence of all these approaches can be explained using this intuitive idea: synchronization is determined by the trade-off between the connectivity of the network and the dissimilarity of the oscillators. Despite being elegant and insightful, these conditions usually provide conservative estimates of the synchronization threshold for large networks.

To get sharp closed-form synchronization tests for coupled oscillators, it is conjectured that instead of comparing the heterogeneity of oscillators with the well-established measures of connectivity such as spectral connectivity or nodal degree, one should focus on mixed measures of connectivity and heterogeneity of the network [11]. Inspired by characterization of frequency synchronization for acyclic networks, a suitable measure of connectivity and heterogeneity is proposed in [11]. Using numerical analysis for several random graphs and IEEE test cases, it has been shown that this condition provides a good estimate of the threshold of synchronization for different classes of graphs. Using cutset projections, a rigorous, more-conservative, and generally-applicable modified version of this test has been established for synchronization in [15].

*This work was supported in part by the U.S. Department of Energy (DOE) Solar Energy Technologies Office under Contract No. DE-EE0000-1583.

¹Department of Mechanical Engineering and the Center of Control, Dynamical Systems and Computation, University of California, Santa Barbara, 93106-5070, USA {eyhuang, saber.jafarpour, bullo}@engineering.ucsb.edu

Contribution: In this paper, we obtain a recursive scheme to compute the Taylor expansion of the inverse Kuramoto map for the network of coupled Kuramoto oscillators with arbitrary topology. Using results from theory of complex analysis in several variables, we find an estimate on the domain of convergence of this Taylor series. We show that this Taylor expansion provides a mathematical explanation for the correct form of the trade-off between the coupling strengths and oscillators heterogeneity for synchronization of coupled oscillators. By truncating the Taylor series, we obtain a family of approximate synchronization tests which can be used to estimate the threshold of synchronization as well as find the approximate position of the synchronization manifold of the network. Using numerical simulations, we show that these approximate tests provide a reasonably-accurate computationally-efficient tool for estimating the synchronization of Kuramoto model.

II. NOTATION

For $n \in \mathbb{Z}_{>0}$, let \mathbb{T}^n denote the n -torus, let $\mathbf{1}_n$ (resp. $\mathbf{0}_n$) denote the vector in \mathbb{R}^n with all entries equal to 1 (resp. 0), and define the vector subspace $\mathbb{1}_n^\perp = \{x \in \mathbb{R}^n \mid \mathbf{1}_n^\top x = 0\}$. Similarly, define the vector subspace $\mathbb{1}_\mathbb{C}^\perp = \{x \in \mathbb{C}^n \mid \mathbf{1}_n^\top x = 0\}$. We denote $\sqrt{-1}$ by i . For every $\mathbf{x} = (x_1, \dots, x_n)^\top \in \mathbb{R}^n$, we define $\exp(i\mathbf{x}) = (e^{ix_1}, \dots, e^{ix_n})^\top \in \mathbb{T}^n$. A set $R \subseteq \mathbb{C}^n$ is a Reinhardt domain, if, for every $(x_1, \dots, x_n)^\top \in \mathbb{R}^n$ and every $(z_1, \dots, z_n)^\top \in R$, we have $(e^{ix_1} z_1, \dots, e^{ix_n} z_n)^\top \in R$. For a complex number $z = x + iy \in \mathbb{C}$, the norm of z is denoted by $\|z\| = \sqrt{x^2 + y^2}$. For a matrix $A = \{a_{ij}\} \in \mathbb{C}^{n \times m}$, the Hermitian of A is denoted by $A^H \in \mathbb{C}^{m \times n}$ and the ∞ -norm of A is defined by $\|A\|_\infty = \max_i \sum_{j=1}^m \|a_{ij}\|$. The Moore–Penrose pseudoinverse of A is the unique $A^\dagger \in \mathbb{C}^{m \times n}$ which satisfies $AA^\dagger A = A$, $A^\dagger AA^\dagger = A^\dagger$, $(AA^\dagger)^H = AA^\dagger$, and $(A^\dagger A)^H = A^\dagger A$. We define the function $\text{sinc} : \mathbb{C} \rightarrow \mathbb{C}$ by

$$\text{sinc}(z) = \begin{cases} \frac{\sin(z)}{z} & z \neq 0, \\ 1 & z = 0. \end{cases}$$

For a complex vector $\mathbf{x} \in \mathbb{C}^n$, we denote the $\text{diag}(\mathbf{x})$ by $[\mathbf{x}]$. For complex vectors $\mathbf{x}, \mathbf{y} \in \mathbb{C}^n$ and we define their Hadamard product by $\mathbf{x} \circ \mathbf{y} = [\mathbf{x}]\mathbf{y} = [\mathbf{y}]\mathbf{x}$. For $n \in \mathbb{Z}_{\geq 0}$, we define the Hadamard power of a complex vector \mathbf{x} by

$$(\mathbf{x})^{\circ n} = \underbrace{[\mathbf{x}] \dots [\mathbf{x}]}_{n-1} \mathbf{x}.$$

We define subspaces $\text{Img}_\mathbb{C}(M) \subseteq \mathbb{C}^m$ and $\text{Ker}_\mathbb{C}(M) \subseteq \mathbb{C}^n$ as follows:

$$\begin{aligned} \text{Img}_\mathbb{C}(M) &= \{\mathbf{x} \in \mathbb{C}^m \mid \exists \mathbf{y} \in \mathbb{C}^n \text{ s.t. } \mathbf{x} = M\mathbf{y}\}, \\ \text{Ker}_\mathbb{C}(M) &= \{\mathbf{x} \in \mathbb{C}^n \mid M\mathbf{x} = \mathbf{0}_m\}. \end{aligned}$$

It is easy to see that the real subspaces $\text{Img}(M)$ and $\text{Ker}(M)$ are the restrictions of the complex subspaces $\text{Img}_\mathbb{C}(M)$ and $\text{Ker}_\mathbb{C}(M)$ to the real Euclidean space, respectively. The number of partitions of the integer $2n + 1$ into $2k + 1$ odd numbers is denoted by $p(k, n)$. An element in $p(k, n)$

is denoted by $\boldsymbol{\alpha} = (\alpha_1, \dots, \alpha_{2k+1})^\top$ where $\sum_{i=1}^{2k+1} \alpha_i = 2n+1$. Let G be a weighted undirected connected graph with the node set $\mathcal{N} = \{1, \dots, n\}$, the edge set $\mathcal{E} \subseteq \mathcal{N} \times \mathcal{N}$, and the adjacency matrix $A \in \mathbb{R}^{n \times n}$. We denote the incidence matrix of G by B and the Laplacian matrix of the graph G by L . It is known that $L = BAB^\top$, where $A \in \mathbb{R}^{m \times m}$ is the diagonal weight matrix defined by $A_{kl} = a_{ij}$ for $k = l = (i, j)$ and 0 otherwise. For every complex vector $\mathbf{w} \in \mathbb{C}^n$, we define $L_{\mathbf{w}} = BA[\mathbf{w}]B^\top$. The cutset projection of G , denoted by \mathcal{P} , is the oblique projection onto the cutset space of G parallel to the cycle space of G [15, Theorem 4]. One can show that $\mathcal{P} = B^\top L^\dagger BA$ [15, Theorem 4]. Additional properties of the cutset projection can be found in [15]. Let T_s be a spanning tree of the graph G . Then we denote the incidence matrix of T_s by $B_s \in \mathbb{R}^{n \times (n-1)}$. We define the matrix $B_s^\# \in \mathbb{R}^{m \times (n-1)}$ by $B_s^\# = (B_s^\dagger B)^\top$. Since T_s is a spanning tree of G , we have $B_s B_s^\dagger B = B$. This implies that $B_s^\# B_s^\top = B^\top$.

III. HETEROGENOUS KURAMOTO MODEL

The Kuramoto model is a system of n oscillators, where each oscillator has a natural frequency $\omega_i \in \mathbb{R}$ and its state is represented by a phase angle $\theta_i \in \mathbb{S}^1$. The interconnection of these oscillators are described using a weighted undirected connected graph G , with nodes $\mathcal{N} = \{1, \dots, n\}$, edges $\mathcal{E} \subseteq \mathcal{N} \times \mathcal{N}$, and positive weights $a_{ij} = a_{ji} > 0$ for all $ij \in \mathcal{E}$. The dynamics for the heterogeneous Kuramoto model is given by:

$$\dot{\theta}_i = \omega_i - \sum_{j=1}^n a_{ij} \sin(\theta_i - \theta_j), \quad \text{for } i \in \{1, \dots, n\}.$$

In matrix language, the Kuramoto model is given by:

$$\dot{\theta} = \omega - BA \sin(B^\top \theta), \quad (1)$$

where $\theta = (\theta_1, \theta_2, \dots, \theta_n)^\top \in \mathbb{T}^n$ is the phase vector, $\omega = (\omega_1, \omega_2, \dots, \omega_n)^\top \in \mathbb{R}^n$ is the natural frequency vector. For every $s \in [0, 2\pi)$, the clockwise rotation of $\theta \in \mathbb{T}^n$ by the angle s is the function $\text{rot}_s : \mathbb{T}^n \rightarrow \mathbb{T}^n$ defined by

$$\text{rot}_s(\theta) = (\theta_1 + s, \dots, \theta_n + s)^\top, \quad \text{for } \theta \in \mathbb{T}^n.$$

Given $\theta \in \mathbb{T}^n$, define the equivalence class $[\theta]$ by

$$[\theta] = \{\text{rot}_s(\theta) \mid s \in [0, 2\pi)\}.$$

The quotient space of \mathbb{T}^n under the above equivalence class is denoted by $[\mathbb{T}^n]$. If $\theta : \mathbb{R}_{\geq 0} \rightarrow \mathbb{T}^n$ is a solution for the Kuramoto model (1) then, for every $s \in [0, 2\pi)$, the curve $\text{rot}_s(\theta) : \mathbb{R}_{\geq 0} \rightarrow \mathbb{T}^n$ is also a solution of (1). A solution $\theta : \mathbb{R}_{\geq 0} \rightarrow \mathbb{T}^n$ of the Kuramoto model (1) achieves *frequency synchronization* if there exists a synchronous frequency $\omega_{\text{syn}} \in \mathbb{R}$ such that

$$\lim_{t \rightarrow \infty} \dot{\theta}(t) = \omega_{\text{syn}} \mathbf{1}_n.$$

By summing all the equations in (1), we obtain $\omega_{\text{syn}} = \frac{1}{n} \left(\sum_{i=1}^n \omega_i \right)$. Therefore, by choosing a rotating frame with frequency ω_{syn} , one can assume that $\omega \in \mathbb{1}_n^\perp$. Given natural

frequency vector $\omega \in \mathbb{1}_n^\perp$, the *synchronization manifold* of the Kuramoto model is given by

$$\omega = BA \sin(B^\top \theta). \quad (2)$$

In many application of the Kuramoto model, such as the power networks, it is not only important to achieve the frequency synchronization but it is also essential that the synchronization manifold satisfies some phase constraints. These constraints can be understood as performance measures for the frequency synchronization. In power network applications, these constraints are usually imposed by the thermal and power capacity of the lines in the network. For every $\gamma \in [0, \frac{\pi}{2})$, we define the *embedded cohesive subset* $S^G(\gamma) \subseteq \mathbb{T}^n$ by

$$S^G(\gamma) = \{\text{rot}_s(\exp(i\mathbf{x})) \mid \mathbf{x} \in D^G(\gamma) \text{ and } s \in [0, 2\pi)\},$$

where $D^G(\gamma) = \{\mathbf{x} \in \mathbb{1}_n^\perp \mid \|B^\top \mathbf{x}\|_\infty \leq \gamma\}$. It can be shown that $S^G(\gamma)$ is diffeomorphic with $D^G(\gamma)$ [15, Theorem 8]. We refer the readers to [15] for further properties of the embedded cohesive subset. In this rest of this paper, we restrict our study to frequency synchronization of the Kuramoto model (1) in the domains $S^G(\gamma)$, for $\gamma \in [0, \frac{\pi}{2})$. We consider the state space of the Kuramoto model (1) to be $[\mathbb{T}^n]$ and we identify the embedded cohesive subset $S^G(\gamma)$ by $D^G(\gamma)$.

IV. SYNCHRONIZATION OF KURAMOTO MODEL

We start by introducing a map which arises naturally in the study of synchronization of the Kuramoto model (1). The *Kuramoto map* $f_K : \mathbb{1}_n^\perp \rightarrow \text{Img}(B^\top)$ is defined by

$$f_K(\mathbf{x}) = \mathcal{P} \sin(B^\top \mathbf{x}). \quad (3)$$

Note that equation (2) can be interpreted as a nodal balance equation. By multiplying both side of equations (2) by $B^\top L^\dagger$, we get

$$B^\top L^\dagger \omega = \mathcal{P} \sin(B^\top \mathbf{x}) = f_K(\mathbf{x}), \quad (4)$$

where $B^\top L^\dagger \omega$ are the edge variables associated to ω and equation (4) can be interpreted as the flow balance equation. It can be shown that the frequency synchronization in $S^G(\gamma)$ can be characterized by solutions of the nodal balance equation or the flow balance equation in $S^G(\gamma)$. The following theorem and its proof can be found in [15, Theorem 10]

Theorem 1 (Algebraic characterization of synchronization): Consider the Kuramoto model (1) with $\gamma \in [0, \frac{\pi}{2})$. Then the following statements are equivalent:

- (i) there exists a unique locally exponentially stable synchronization manifold \mathbf{x}^* for the Kuramoto model (1) in $S^G(\gamma)$;
- (ii) there exists a unique solution \mathbf{x}^* for the node balance equation (2) in $S^G(\gamma)$;
- (iii) there exists a unique solution \mathbf{x}^* for the flow balance equation (4) in $S^G(\gamma)$;

Therefore, instead of studying frequency synchronization in $S^G(\gamma)$, we focus on studying the range of the Kuramoto map (3). The following theorem shows that the Kuramoto

map is invertible on the domain $S^G(\gamma)$ and presents an iterative procedure to compute the Taylor expansion of $f_K^{-1}(\eta)$ around $\eta = \mathbf{0}_m$.

Theorem 2 (Inverse Kuramoto map): Consider the Kuramoto map defined in (3). Let $\gamma \in [0, \frac{\pi}{2})$. Then the following statements hold:

- (i) there exists a real analytic bijective function $f_K^{-1} : f_K(S^G(\gamma)) \rightarrow S^G(\gamma)$ such that

$$\begin{aligned} f_K^{-1} \circ f_K(\mathbf{x}) &= \mathbf{x}, & \text{for } \mathbf{x} \in S^G(\gamma), \\ f_K \circ f_K^{-1}(\eta) &= \eta, & \text{for } \eta \in f_K(S^G(\gamma)); \end{aligned}$$

- (ii) the map $B^\top f_K^{-1}(\eta)$ has the following Taylor expansion around $\eta = \mathbf{0}_m$:

$$\sum_{j=0}^{\infty} A_{2j+1}(\eta), \quad (5)$$

where $A_{2j+1}(\eta)$ is a homogeneous polynomial of order $2j+1$ in η computed iteratively by:

$$\begin{aligned} A_1(\eta) &= \eta, \\ A_{2j+1}(\eta) &= \mathcal{P} \left(\sum_{k=1}^j \frac{(-1)^{k+1}}{(2k+1)!} \sum_{\alpha \in p(k,n)} A_\alpha(\eta) \right), \end{aligned}$$

where, for $\alpha = (\alpha_1, \dots, \alpha_{2k+1}) \in p(k, n)$, we denote $A_\alpha(\eta) = A_{\alpha_1}(\eta) \circ \dots \circ A_{\alpha_{2k+1}}(\eta)$.

Proof: Regarding part (i), we first show that f_K is a local diffeomorphism on $S^G(\gamma)$. Note that, for every $\mathbf{x} \in S^G(\gamma)$, we have $D_{\mathbf{x}} f_K = \mathcal{P}[\cos(B^\top \mathbf{x})] B^\top$. Suppose that $v \in \mathbb{1}_n$ is such that $D_{\mathbf{x}} f_K(v) = \mathbf{0}_n$. This implies that $[\cos(B^\top \mathbf{x})] B^\top(v) \in \text{Ker}(\mathcal{P}) = \text{Ker}(BA)$ and therefore

$$v^\top BA[\cos(B^\top \mathbf{x})] B^\top(v) = 0.$$

Since $\mathbf{x} \in S^G(\gamma)$, we have $\cos(x_i - x_j) > 0$, for every $(i, j) \in \mathcal{E}$. Thus, the matrix $BA[\cos(B^\top \mathbf{x})] B^\top$ is positive semidefinite with $\mathbb{1}_n$ being the only eigenvector associated to the eigenvalue 0. This implies that $v = \mathbf{0}_n$. Therefore, for every $\mathbf{x} \in S^G(\gamma)$, the map $D_{\mathbf{x}} f_K$ is an isomorphism. The Inverse Function Theorem [1, Theorem 2.5.2] implies that f_K is a local diffeomorphism. Now we show that f_K is one-to-one on the domain $S^G(\gamma)$. Suppose that $\mathbf{x}_1, \mathbf{x}_2 \in S^G(\gamma)$ are such that $f_K(\mathbf{x}_1) = f_K(\mathbf{x}_2)$. This means that $BA \sin(B^\top \mathbf{x}_1) = BA \sin(B^\top \mathbf{x}_2)$. As a result, we have

$$\begin{aligned} 0 &= (\mathbf{x}_1 - \mathbf{x}_2)^\top BA(\sin(B^\top \mathbf{x}_1) - \sin(B^\top \mathbf{x}_2)) \\ &= (B^\top \mathbf{x}_1 - B^\top \mathbf{x}_2)^\top \mathcal{A}(\sin(B^\top \mathbf{x}_1) - \sin(B^\top \mathbf{x}_2)). \end{aligned}$$

Since the function $y \mapsto \sin(y)$ is strictly increasing on the interval $(-\frac{\pi}{2}, \frac{\pi}{2})$, we get $B^\top \mathbf{x}_1 = B^\top \mathbf{x}_2$. This implies that $\mathbf{x}_1 = \mathbf{x}_2$ and the function f_K is one-to-one on $S^G(\gamma)$. Note that an injective local diffeomorphism with compact domain is a diffeomorphism onto its image [20, Proposition 7.4]. Therefore, the map $f_K : S^G(\gamma) \rightarrow f_K(S^G(\gamma))$ is a global diffeomorphism and part (i) follows from this result.

Regarding part (ii), suppose that $\sum_{j=0}^{\infty} A_j(\eta)$ is the Taylor expansion of $B^\top f_{\mathbf{K}}^{-1}(\eta)$ around $\eta = \mathbb{0}_m$. Then we have

$$\begin{aligned} \eta &= f_{\mathbf{K}} \circ f_{\mathbf{K}}^{-1}(\eta) = \mathcal{P} \sin(B^\top f_{\mathbf{K}}^{-1}(\eta)) \\ &= \mathcal{P} \sum_{k=0}^{\infty} \frac{(-1)^k}{(2k+1)!} \left(\sum_{i=0}^{\infty} A_i(\eta) \right)^{\circ(2k+1)} \end{aligned}$$

By equating the same order terms on both side of the above equality, we get $A_1(\eta) = \eta$. Moreover, for every $j \in \mathbb{Z}_{\geq 0}$, we get $A_{2j}(\eta) = \mathbb{0}_m$. For the odd order terms we get

$$A_{2j+1}(\eta) = \mathcal{P} \left(\sum_{k=1}^j \frac{(-1)^{k+1}}{(2k+1)!} \sum_{\alpha \in \mathcal{P}(k,n)} A_\alpha(\eta) \right).$$

This completes the proof of the theorem. \blacksquare

Remark 3: 1) One can compute the first five terms in the Taylor series (5) as follows:

$$\begin{aligned} A_1(\eta) &= \eta, \quad A_3(\eta) = \mathcal{P} \left(\frac{1}{3!} (\eta)^{\circ 3} \right), \\ A_5(\eta) &= \mathcal{P} \left(\frac{3}{3!} A_3(\eta) \circ (\eta)^{\circ 2} - \frac{1}{5!} (\eta)^{\circ 5} \right), \\ A_7(\eta) &= \mathcal{P} \left(\frac{3}{3!} A_5(\eta) \circ (\eta)^{\circ 2} + \frac{3}{3!} (A_3(\eta))^{\circ 2} \circ \eta \right. \\ &\quad \left. - \frac{5}{5!} A_3(\eta) \circ (\eta)^{\circ 4} + \frac{1}{7!} (\eta)^{\circ 7} \right). \end{aligned}$$

2) Using Theorem 2(ii), it is easy to see that the Taylor expansion for $f_{\mathbf{K}}^{-1}(\eta)$ is given by $\sum_{j=0}^{\infty} B_{2j+1}(\eta)$, where we have $B_{2j+1}(\eta) = L^\dagger B \mathcal{A}(A_{2j+1}(\eta))$, for every $j \in \mathbb{Z}_{\geq 0}$. \square

Before we state the main result of this paper, it is convenient to introduce the smooth function $g : [1, \infty) \rightarrow \mathbb{R}$ defined by

$$g(x) = \frac{y(x) + \sin(y(x))}{2} - x \frac{y(x) - \sin(y(x))}{2} \Big|_{y(x) = \arccos\left(\frac{x-1}{x+1}\right)}.$$

One can verify that $g(1) = 1$, g is monotonically decreasing, and $\lim_{x \rightarrow \infty} g(x) = 0$; the graph of g is shown in Figure 1. Suppose that G is a weighted undirected connected graph

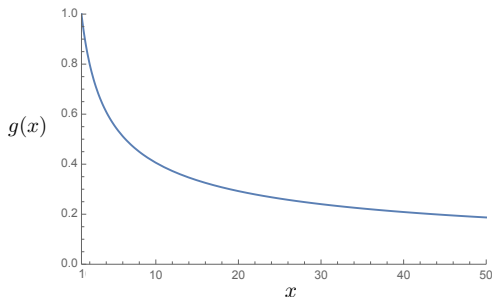


Fig. 1: The graph of the monotonically-decreasing function g

and T_s is a spanning tree of G . Then using function g , one

can define two subsets of $\text{Img}(B^\top)$ as follows:

$$\begin{aligned} \Omega &= \{\eta \in \text{Img}(B^\top) \mid \|\eta\|_\infty \leq g(\|\mathcal{P}\|_\infty)\}, \\ \Omega^s &= \{\xi \in \text{Img}(B_s^\top) \mid \|\xi\|_\infty \leq \|B_s^\# \|_\infty^{-1} g(\|\mathcal{P}\|_\infty)\}, \end{aligned}$$

It is clear that we have $B_s^\# \Omega^s \subseteq \Omega$. In order to study the convergence of the Taylor series (5), we need to use various tools from theory of complex analysis in several variables. These tools are developed in the Appendix. In the next theorem, using the results in the Appendix, we prove the convergence of the Taylor expansion (5) on a suitable domain.

Theorem 4 (Synchronization of Kuramoto model):

Consider the Kuramoto model (1), with graph G and cutset projection \mathcal{P} . Suppose that T_s is a spanning tree of G and define $\gamma^* \in [0, \frac{\pi}{2})$ by

$$\gamma^* = \arccos \left(\frac{\|\mathcal{P}\|_\infty - 1}{\|\mathcal{P}\|_\infty + 1} \right).$$

Then the following statements holds:

- (i) For every $\omega \in \mathbb{1}_n^\perp$ such that $B^\top L^\dagger \omega \in \Omega$, there exists a unique locally exponentially stable synchronization manifold \mathbf{x}^* for the Kuramoto model (1) in $S^G(\gamma^*)$;
- (ii) For every $\omega \in \mathbb{1}_n^\perp$ such that $B_s^\top L^\dagger \omega \in \Omega^s$, the Taylor expansion (5):

$$\sum_{j=0}^{\infty} A_{2j+1}(B^\top L^\dagger \omega)$$

converges absolutely to $B^\top \mathbf{x}^*$.

Proof: Regarding part (i), by Theorem 9(ii), there exists $\mathbf{x}^* \in S^G(\gamma^*)$ such that $B^\top L^\dagger \omega = f_{\mathbf{K}}(\mathbf{x}^*)$. The result follows from Theorem 1(iii).

Regarding part (ii), we use the notations and results in the Appendix. First note that by Theorem 10(ii), the inverse of the complex Kuramoto map $f_{\mathbf{K}\mathbb{C}}^{-1}$ is a well-defined holomorphic diffeomorphism on $\Omega_{\mathbb{C}}$. It is easy to see that $B_s^\# \Omega_{\mathbb{C}}^s \subseteq \Omega_{\mathbb{C}}$. Therefore, one can define the holomorphic mapping $B^\top f_{\mathbf{K}\mathbb{C}}^{-1} \circ B_s^\# : \Omega_{\mathbb{C}}^s \rightarrow \text{Img}_{\mathbb{C}}(B^\top)$ by

$$B^\top f_{\mathbf{K}\mathbb{C}}^{-1} \circ B_s^\#(\mathbf{x}) = B^\top f_{\mathbf{K}\mathbb{C}}^{-1}(B_s^\#(\mathbf{x})).$$

It is easy to see that $\sum_{j=0}^{\infty} A_{2j+1}(B_s^\#(\mathbf{x}))$ is the Taylor expansion of the mapping $B^\top f_{\mathbf{K}\mathbb{C}}^{-1} \circ B_s^\#(\mathbf{x})$ around $\mathbf{x} = \mathbb{0}_{n-1}$. Moreover, the set $\Omega_{\mathbb{C}}^s$ is a Reinhardt domain in \mathbb{C}^{n-1} . Therefore, by [13, Theorem 2.4.5], the Taylor series $\sum_{j=0}^{\infty} A_{2j+1}(B_s^\#(\mathbf{x}))$ converges absolutely to $B^\top f_{\mathbf{K}\mathbb{C}}^{-1} \circ B_s^\#(\mathbf{x})$, for every $\mathbf{x} \in \Omega_{\mathbb{C}}^s$. Since $B_s^\top L^\dagger \omega \in \Omega_{\mathbb{C}}^s$, the Taylor series

$$\sum_{j=0}^{\infty} A_{2j+1}(B_s^\#(B_s^\top L^\dagger \omega)) = \sum_{j=0}^{\infty} A_{2j+1}(B^\top L^\dagger \omega)$$

converges absolutely to $B^\top f_{\mathbf{K}\mathbb{C}}^{-1} \circ B_s^\#(B_s^\top L^\dagger \omega) = B^\top f_{\mathbf{K}\mathbb{C}}^{-1}(B^\top L^\dagger \omega) = B^\top \mathbf{x}^*$. \blacksquare

Theorem 4(ii) provides an estimate on the domain of convergence of the power series (5). For many large networks, this estimate is overly conservative and the domain of

convergence is usually much larger than Ω^s . However, one can still use the formal power series (5) as a tool for studying approximate synchronization of the Kuramoto model as well as the approximate position of the synchronization manifold.

Definition 5 (Approximate synchronization): For $n \in \mathbb{Z}_{\geq 0}$, we define the $(2n+1)$ th approximate synchronization manifold $S_{2n+1} \in \mathbb{1}_n^\perp$ of the Kuramoto model (1) by

$$S_{2n+1} = L^\dagger B A \left(\sum_{j=1}^n A_{2j+1} (B^\top L^\dagger \omega) \right), \quad (6)$$

and the $(2n+1)$ th approximate synchronization test T_{2n+1} for synchronization of the Kuramoto model (1) in $S^G(\gamma)$ by

$$\left\| \sum_{j=1}^n A_{2j+1} (B^\top L^\dagger \omega) \right\|_\infty \leq \gamma. \quad (7)$$

V. SIMULATIONS

In this section, we study the accuracy and computational time of the family of approximate tests (6) and (7) on several IEEE test cases. An IEEE test case is described by a connected graph G and a nodal admittance matrix $Y \in \mathbb{C}^{n \times n}$. The set of nodes of G is partitioned into a set of load buses \mathcal{N}_1 and a set of generator buses \mathcal{N}_2 . The voltage at the node $j \in \mathcal{N}_1 \cup \mathcal{N}_2$ is denoted by V_j , where $V_j = |V_j| e^{i\theta_j}$ and the power demand (resp. power injection) at node $j \in \mathcal{N}_1$ (resp. $j \in \mathcal{N}_2$) is denoted by P_j . By ignoring the resistances in the network and the power balance equations for reactive power, the synchronization manifold [11] of the network satisfies the following Kuramoto model [11]:

$$P_j - \sum_{l \in \mathcal{N}_1 \cup \mathcal{N}_2} a_{jl} \sin(\theta_j - \theta_l) = 0, \quad \forall j \in \mathcal{N}_1 \cup \mathcal{N}_2. \quad (8)$$

where $a_{jl} = a_{lj} = |V_j| |V_l| \text{Im}(Y_{jl})$, for connected nodes j and l . We consider effective power injections (demands) to be a scalar multiplication of nominal power injections (demands), i.e., given nominal power profile P^{nom} we set $P_j = K P_j^{\text{nom}}$, for some $K \in \mathbb{R}_{>0}$ and for every $j \in \mathcal{N}_1 \cup \mathcal{N}_2$. The voltage magnitudes at the generator buses are pre-determined and the voltage magnitudes at load buses are computed by solving the reactive power balance equations using the optimal power flow solver provided by MATPOWER [31]. For six IEEE test cases given in Table I, we numerically compute the accuracy of the approximate synchronization test T_5 in the domains $S^G(\pi/4)$ and $S^G(\pi/2)$.

- Remark 6:**
- 1) By increasing the value of γ , the accuracy of the approximate tests decreases;
 - 2) By increasing the number of nodes in the IEEE test case, the computation time of the approximate test increases. This is mainly because computing the approximate test requires multiplication by the matrix $\mathcal{P} \in \mathbb{R}^{m \times m}$ which is a dense matrix with $n-1 \leq m \leq \binom{n}{2}$. \square

For a select set of the IEEE test cases, we compute the accuracy of equations (6) in approximating the position of the

Test Case	T_5 for $\gamma = \frac{\pi}{4}$		T_5 for $\gamma = \frac{\pi}{2}$	
	Accuracy*	Computation time †	Accuracy	Computation time
Chow 9	99.57 %	0.51 %	90.05 %	0.48 %
IEEE 14	99.80 %	0.26 %	94.96 %	0.43 %
IEEE 30	99.80 %	0.64 %	93.84 %	0.82 %
IEEE 57	99.80 %	0.83 %	94.77 %	1.67 %
IEEE 118	99.69 %	2.47 %	93.60 %	4.39 %
IEEE 300	99.42 %	10.60 %	84.46 %	17.55 %

* Accuracy is compared with the solution of *fsolve*.

† Computation time is compared with the computation time of *fsolve*.

TABLE I: Comparison of accuracy and computation time of approximate synchronization test T_5 on six IEEE test cases.

synchronization manifold of the system. For every $n \in \mathbb{Z}_{\geq 0}$, we define the error of the approximate manifold S_{2n+1} by

$$E_{2n+1} = \|S_{2n+1} - \theta^*\|_\infty$$

where $\theta^* \in \mathbb{1}_n^\perp$ is the solution for the power flow equations (8) using *fsolve* in MATLAB. The comparison of the error for different approximate manifolds is shown in Figure (2).

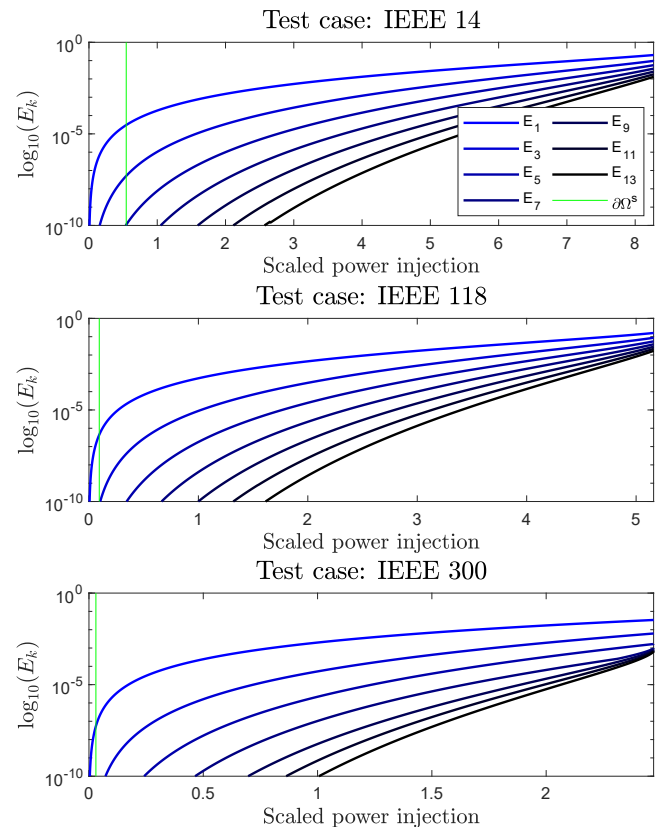


Fig. 2: Comparison of accuracy of the approximate synchronization manifold S_{2n+1} for select IEEE test cases. The green line in these graphs shows the boundary of the region Ω^s .

VI. CONCLUSION

We presented an algorithm to compute the Taylor expansion of the inverse Kuramoto map. We showed that this Taylor series can be used to study the frequency synchronization

as well as to find the position of the synchronization manifold of the Kuramoto model of coupled oscillators. Using techniques from complex analysis in several variable, we found an estimate on the domain of convergence of this Taylor series. Numerical simulations show that this power series gives approximations of the synchronization of Kuramoto model with reasonable accuracy and low computational cost, way beyond our estimate on its domain of convergence.

APPENDIX

In this appendix, we generalize the results in [15] to the complexified Kuramoto model. We start by defining the domains

$$\begin{aligned} S_{\mathbb{C}}^G(\gamma) &= \{\mathbf{x} \in \mathbb{1}_{\mathbb{C}}^\perp \mid \|B^\top \mathbf{x}\|_\infty \leq \gamma\}, \\ \Omega_{\mathbb{C}} &= \{\eta \in \text{Im}g_{\mathbb{C}}(B^\top) \mid \|\eta\|_\infty \leq g(\|\mathcal{P}\|_\infty)\}, \\ \Omega_{\mathbb{C}}^s &= \{\xi \in \text{Im}g_{\mathbb{C}}(B_s^\top) \mid \|\xi\|_\infty \leq \|B_s^\# \|_\infty^{-1} g(\|\mathcal{P}\|_\infty)\}, \end{aligned}$$

and complex Kuramoto map $f_{\text{KC}} : \mathbb{1}_{\mathbb{C}}^\perp \rightarrow \text{Im}g_{\mathbb{C}}(B^\top)$ by

$$f_{\text{KC}}(\mathbf{z}) = \mathcal{P} \sin(B^\top \mathbf{z}). \quad (9)$$

We first state a useful lemma.

Lemma 7: Let $\mathbf{z} \in S_{\mathbb{C}}^G(\frac{\pi}{2})$. Then we have

$$\text{rank}(L_{\cos(\mathbf{z})}) = \text{rank}(L_{\text{sinc}(\mathbf{z})}) = n - 1.$$

Proof: Let $\mathbf{w} \in \mathbb{C}^n$. Then it is clear that $L_{\mathbf{w}} \mathbb{1}_n = \mathbb{0}_n$. Suppose that, for some $v \in \mathbb{1}_{\mathbb{C}}^\perp$, we have $L_{\mathbf{w}} v = \mathbf{0}$. This implies that $BA[\mathbf{w}]B^\top v = \mathbb{0}_n$. Therefore, we have $v^H BA[\mathbf{w}]B^\top v = \mathbb{0}_n$. Since B and \mathcal{A} are real matrices, we have

$$\text{Re}(v^H BA[\mathbf{w}]B^\top v) = v^H BA[\text{Re}(\mathbf{w})]B^\top v = \mathbb{0}_n.$$

Suppose that $\mathbf{z} = \mathbf{x} + i\mathbf{y}$. If we set $\mathbf{w} = \cos(\mathbf{z})$, then $\text{Re}(\mathbf{w}) = [\cos(\mathbf{x})] \cosh(\mathbf{y})$. Therefore, for every $z \in S_{\mathbb{C}}^G(\frac{\pi}{2})$, the matrix $BA[\cos(B^\top \mathbf{x})][\cosh(B^\top \mathbf{y})]B^\top$ is positive semidefinite and its only eigenvector associated to the eigenvalue 0 is $\mathbb{1}_n$. Thus $v \in \text{span}_{\mathbb{C}}(\mathbb{1}_n)$ and we have $\text{rank}(L_{\cos(\mathbf{z})}) = n - 1$. If we set $\mathbf{w} = \text{sinc}(\mathbf{z})$, then we know that, for every $i \in \{1, \dots, m\}$, we have

$$\begin{aligned} \text{Re}(\text{sinc}(z_i)) &= \frac{x_i \sin(x_i) \cosh(y_i) + y_i \cos(x_i) \sinh(y_i)}{\sqrt{x_i^2 + y_i^2}}. \end{aligned}$$

Therefore, for every $\mathbf{z} \in S_{\mathbb{C}}^G(\frac{\pi}{2})$, the matrix $BA[\text{Re}(\text{sinc}(\mathbf{z}))]B^\top$ is positive semidefinite and its only eigenvector associated to the eigenvalue 0 is $\mathbb{1}_n$. Thus $v \in \text{span}_{\mathbb{C}}(\mathbb{1}_n)$ and we have $\text{rank}(L_{\text{sinc}(\mathbf{z})}) = n - 1$. ■

For every $\mathbf{y} \in \text{Im}g_{\mathbb{C}}(B^\top)$, we define the map $Q_{\mathbf{y}} : \text{Im}g_{\mathbb{C}}(B^\top) \rightarrow \text{Im}g_{\mathbb{C}}(B^\top)$ by

$$Q_{\mathbf{y}} \mathbf{x} = \mathcal{P}[\text{sinc}(\mathbf{y})] \mathbf{x}, \quad \text{for all } \mathbf{x} \in \text{Im}g_{\mathbb{C}}(B^\top).$$

Then we have the following lemma.

Lemma 8: Suppose that $\mathbf{z} \in \text{Im}g_{\mathbb{C}}(B^\top)$ is such that $\|\mathbf{z}\|_\infty \leq \frac{\pi}{2}$, then the following statements hold:

- (i) the map $Q_{\mathbf{z}}$ is invertible;
- (ii) we have $Q_{\mathbf{z}}^{-1} = B^\top L_{\text{sinc}(\mathbf{z})}^\dagger BA$;

(iii) the map $\mathbf{z} \rightarrow Q_{\mathbf{z}}^{-1}$ is continuous on $\|\mathbf{z}\|_\infty \leq \frac{\pi}{2}$.

Proof: Regarding part (i), to show that $Q_{\mathbf{z}}$ is invertible, it suffices to show that it is injective and surjective. We first show that $Q_{\mathbf{z}}$ is injective. Suppose that there exists $v \in \text{Im}g_{\mathbb{C}}(B^\top)$ such that $Q_{\mathbf{z}} v = \mathbb{0}_n$. Let $w \in \mathbb{1}_{\mathbb{C}}^\perp$ be such that $B^\top w = v$. Using the fact that $\text{Ker}_{\mathbb{C}}(\mathcal{P}) = \text{Ker}_{\mathbb{C}}(BA)$, we get

$$BA[\text{sinc}(\mathbf{z})]B^\top w = \mathbb{0}_n.$$

Using Lemma 7, we get $w = \mathbb{0}_n$ and $v = \mathbb{0}_n$. The surjective of $Q_{\mathbf{z}}$ follows from Rank-nullity Theorem.

Regarding part (ii), for every $v \in \text{Im}g_{\mathbb{C}}(B^\top)$, we have

$$Q_{\mathbf{z}} B^\top L_{\text{sinc}(\mathbf{z})}^\dagger BA v = \mathcal{P}[\text{sinc}(\mathbf{z})] B^\top L_{\text{sinc}(\mathbf{z})}^\dagger BA v$$

Using Lemma 7, $\text{rank}(L_{\text{sinc}(\mathbf{z})}) = n - 1$. This implies that $L_{\text{sinc}(\mathbf{z})}^\dagger L_{\text{sinc}(\mathbf{z})} = L_{\text{sinc}(\mathbf{z})} L_{\text{sinc}(\mathbf{z})}^\dagger = I_n - \frac{1}{n} \mathbb{1}_n \mathbb{1}_n^\top$. Therefore

$$Q_{\mathbf{z}} B^\top L_{\text{sinc}(\mathbf{z})}^\dagger BA v = B^\top L_{\text{sinc}(\mathbf{z})}^\dagger BA v = v.$$

Using part (i), one can deduce that $Q_{\mathbf{z}}^{-1} = B^\top L_{\text{sinc}(\mathbf{z})}^\dagger BA$.

Regarding part (iii), the result follows from part (ii) and [24, Theorem 4.2]. ■

Now we can prove the main result of this appendix.

Theorem 9 (Range of the complex Kuramoto map):

Define $\gamma^* \in [0, \frac{\pi}{2})$ by

$$\gamma^* = \arccos\left(\frac{\|\mathcal{P}\|_\infty - 1}{\|\mathcal{P}\|_\infty + 1}\right).$$

and suppose that $\eta \in \text{Im}g_{\mathbb{C}}(B^\top)$ is such that

$$\|\eta\|_\infty \leq g(\|\mathcal{P}\|_\infty).$$

Then the following statements hold:

- (i) There exists a unique $\mathbf{z}^* \in S_{\mathbb{C}}^G(\gamma^*)$ such that $\eta = f_{\text{KC}}(\mathbf{z}^*)$;
- (ii) If $\eta \in \mathbb{R}^m$, then there exists a unique $\mathbf{x}^* \in S^G(\gamma^*)$ such that $\eta = f_{\text{KC}}(\mathbf{x}^*)$;

Proof: Regarding part (i), define the set $\Gamma = \{\mathbf{x} \in \text{Im}g_{\mathbb{C}}(B^\top) \mid \|\mathbf{x}\|_\infty \leq \gamma^*\}$. Then one can consider the following fixed-point problem on Γ :

$$\mathbf{y} = Q_{\mathbf{z}}^{-1}(\eta) := h_\eta(\mathbf{z}). \quad (10)$$

By Lemma 8, the map $\mathbf{z} \rightarrow h_\eta(\mathbf{z})$ is well-defined and continuous on Γ . We show that $h_\eta(\Gamma) \subseteq \Gamma$. Let $\mathbf{z} \in \Gamma$. Then we have

$$\|h_\eta(\mathbf{z})\|_\infty = \|Q_{\mathbf{z}}^{-1}(\eta)\|_\infty \leq \|Q_{\mathbf{z}}^{-1}\|_\infty \|\eta\|_\infty.$$

By [15, Lemma 24], we have

$$\|Q_{\mathbf{z}}^{-1}\|_\infty = \left(\min_{\mathbf{z} \in \Gamma} \min_{\substack{\mathbf{x} \in \text{Im}g_{\mathbb{C}}(B^\top), \\ \|\mathbf{x}\|_\infty = 1}} \|Q_{\mathbf{z}} \mathbf{x}\|_\infty \right)^{-1}.$$

Let $\mathbf{z} \in \Gamma$, $\mathbf{x} \in \text{Im}g_{\mathbb{C}}(B^\top)$ be such that $\|\mathbf{x}\|_\infty = 1$, and $\mathbf{w} = \text{sinc}(\gamma^*) \mathbb{1}_n$. Then we have

$$\begin{aligned} \|Q_{\mathbf{y}} \mathbf{x}\|_\infty &= \|\mathcal{P}[\text{sinc}(\mathbf{z})] \mathbf{x}\|_\infty \\ &\geq \|\mathcal{P}[\mathbf{w}] \mathbf{x}\|_\infty - \|\mathcal{P}[\mathbf{w} - \text{sinc}(\mathbf{z})] \mathbf{x}\|_\infty. \end{aligned}$$

The first term on the right hand side is given by:

$$\|\mathcal{P}[\mathbf{w}]\mathbf{x}\|_\infty = \frac{1 + \text{sinc}(\gamma^*)}{2}$$

The second term on the right hand side can be bounded as:

$$\|\mathcal{P}[\mathbf{w} - \text{sinc}(\mathbf{z})]\mathbf{x}\|_\infty \leq \|\mathcal{P}\|_\infty \|\mathbf{w} - \text{sinc}(\mathbf{z})\|_\infty$$

Note that, if $\mathbf{z} = \mathbf{x} + i\mathbf{y}$, then we have

$$\begin{aligned} & \|\mathbf{w} - \text{sinc}(\mathbf{z})\|_\infty \\ &= \max_i \left| \frac{1 + \text{sinc}(\gamma^*)}{2} - \frac{\sin(x_i)^2 + \sinh(y_i)^2}{\sqrt{x_i^2 + y_i^2}} \right|. \end{aligned}$$

Therefore,

$$\|\mathcal{P}[\mathbf{w} - \text{sinc}(\mathbf{z})]\mathbf{x}\|_\infty \leq \|\mathcal{P}\|_\infty \frac{1 - \text{sinc}(\gamma^*)}{2}$$

This implies that

$$\begin{aligned} & \min_{\mathbf{z} \in \Gamma} \min_{\substack{\mathbf{x} \in \text{Im}g_{\mathbb{C}}(B^\top), \\ \|\mathbf{x}\|_\infty = 1}} \|Q_{\mathbf{z}}\mathbf{x}\|_\infty \\ & \geq \frac{1 + \text{sinc}(\gamma^*)}{2} - \|\mathcal{P}\|_\infty \frac{1 - \text{sinc}(\gamma^*)}{2} \\ & = \frac{g(\|\mathcal{P}\|_\infty)}{\gamma^*}, \end{aligned}$$

where the last equality is by definition of function g . Thus

$$\|h_\eta(\mathbf{z})\|_\infty \leq \|Q_{\mathbf{z}}^{-1}\|_\infty \|\eta\|_\infty \leq \gamma^*.$$

Therefore, by the Brouwer Fixed-point Theorem, the map h_η has a fixed point in Γ , i.e., there exists $\mathbf{y}^* \in \Gamma$ such that

$$\mathbf{y}^* = h_\eta(\mathbf{y}^*) = Q_{\mathbf{y}^*}^{-1}\eta.$$

This means that we have

$$\eta = Q_{\mathbf{y}^*}\mathbf{y}^* = \mathcal{P} \sin(\mathbf{y}^*).$$

Since $\mathbf{y}^* \in \Gamma$, there exists $\mathbf{z}^* \in S_{\mathbb{C}}^G(\gamma^*)$ such that $\mathbf{y}^* = B^\top \mathbf{z}^*$. This completes the proof of part (i).

Regarding part (ii), the proof is given in [15, Theorem 16 (ii)]. \blacksquare

Using Theorem 9, one can show that the complex Kuramoto map f_{KC} is a diffeomorphism on $\Omega_{\mathbb{C}}$.

Theorem 10 (Inverse complex Kuramoto map):

Consider the complex Kuramoto map defined in (9). Let $\gamma \in [0, \frac{\pi}{2})$. Then the following statements hold:

- (i) $D_{\mathbf{z}}f_{\text{KC}}$ is invertible, for every $\mathbf{z} \in S_{\mathbb{C}}^G(\gamma)$;
- (ii) There exists a holomorphic bijective function $f_{\text{KC}}^{-1} : \Omega_{\mathbb{C}} \rightarrow f_{\text{KC}}^{-1}(\Omega_{\mathbb{C}})$ such that

$$\begin{aligned} f_{\text{KC}}^{-1} \circ f_{\text{KC}}(\mathbf{x}) &= \mathbf{x}, & \text{for } \mathbf{x} \in f_{\text{KC}}^{-1}(\Omega_{\mathbb{C}}), \\ f_{\text{KC}} \circ f_{\text{KC}}^{-1}(\eta) &= \eta, & \text{for } \eta \in \Omega_{\mathbb{C}}; \end{aligned}$$

Proof: Regarding part (i), pick $\mathbf{z} \in S_{\mathbb{C}}^G(\gamma)$. First note that, we have

$$D_{\mathbf{z}}f_{\text{KC}} = \mathcal{P}[\cos(B^\top \mathbf{z})]B^\top.$$

Since $\text{Im}g_{\mathbb{C}}(\mathcal{P}) = \text{Im}g_{\mathbb{C}}(B^\top)$, we know that $\text{rank}(D_{\mathbf{z}}f_{\text{KC}}) = \text{rank}(L_{\cos(\mathbf{z})})$. The result then follows from Lemma 7.

Regarding part (ii), the restriction of the function f_{KC} to the open set $f_{\text{KC}}^{-1}(\Omega_{\mathbb{C}})$ is a holomorphic map $f_{\text{KC}}|_{f_{\text{KC}}^{-1}(\Omega_{\mathbb{C}})} : f_{\text{KC}}^{-1}(\Omega_{\mathbb{C}}) \rightarrow \Omega_{\mathbb{C}}$. Note that $\Omega_{\mathbb{C}} \subseteq S_{\mathbb{C}}^G(\gamma^*)$. Therefore, by part (i), the map f_{KC} is a local holomorphic diffeomorphism at every point in $f_{\text{KC}}^{-1}(\Omega_{\mathbb{C}})$. Moreover, the set $f_{\text{KC}}^{-1}(\Omega_{\mathbb{C}})$ is compact. Therefore, by [20, Proposition 2.19], the map $f_{\text{KC}}|_{f_{\text{KC}}^{-1}(\Omega_{\mathbb{C}})}$ is a covering map. Since the set $\Omega_{\mathbb{C}}$ is simply connected, by [20, Proposition A.28], the mapping $f_{\text{KC}}|_{f_{\text{KC}}^{-1}(\Omega_{\mathbb{C}})}$ is a holomorphic diffeomorphism. Part (ii) of the theorem then follows from this result. \blacksquare

REFERENCES

- [1] R. Abraham, J. E. Marsden, and T. S. Ratiu. *Manifolds, Tensor Analysis, and Applications*, volume 75 of *Applied Mathematical Sciences*. Springer, 2 edition, 1988.
- [2] J. A. Acebrón, L. L. Bonilla, C. J. P. Vicente, F. Ritort, and R. Spigler. The Kuramoto model: A simple paradigm for synchronization phenomena. *Reviews of Modern Physics*, 77(1):137–185, 2005. doi:10.1103/RevModPhys.77.137.
- [3] D. Aeyels and J. A. Rogge. Existence of partial entrainment and stability of phase locking behavior of coupled oscillators. *Progress of Theoretical Physics*, 112(6):921–942, 2004. doi:10.1143/PTP.112.921.
- [4] A. Araposthatis, S. Sastry, and P. Varaiya. Analysis of power-flow equation. *International Journal of Electrical Power & Energy Systems*, 3(3):115–126, 1981. doi:10.1016/0142-0615(81)90017-X.
- [5] A. Arenas, A. Díaz-Guilera, J. Kurths, Y. Moreno, and C. Zhou. Synchronization in complex networks. *Physics Reports*, 469(3):93–153, 2008. doi:10.1016/j.physrep.2008.09.002.
- [6] E. Brown, J. Moehlis, and P. Holmes. On the phase reduction and response dynamics of neural oscillator populations. *Neural Computation*, 16(4):673–715, 2004. doi:10.1162/089976604322860668.
- [7] M. C. Chandorkar, D. M. Divan, and R. Adapa. Control of parallel connected inverters in standalone AC supply systems. *IEEE Transactions on Industry Applications*, 29(1):136–143, 1993. doi:10.1109/28.195899.
- [8] N. Chopra and M. W. Spong. On exponential synchronization of Kuramoto oscillators. *IEEE Transactions on Automatic Control*, 54(2):353–357, 2009. doi:10.1109/TAC.2008.2007884.
- [9] F. Dörfler and F. Bullo. Synchronization and transient stability in power networks and non-uniform Kuramoto oscillators. *SIAM Journal on Control and Optimization*, 50(3):1616–1642, 2012. doi:10.1137/110851584.
- [10] F. Dörfler and F. Bullo. Synchronization in complex networks of phase oscillators: A survey. *Automatica*, 50(6):1539–1564, 2014. doi:10.1016/j.automatica.2014.04.012.
- [11] F. Dörfler, M. Chertkov, and F. Bullo. Synchronization in complex oscillator networks and smart grids. *Proceedings of the National Academy of Sciences*, 110(6):2005–2010, 2013. doi:10.1073/pnas.1212134110.
- [12] A. Franci, A. Chaillet, and W. Pasillas-Lépine. Phase-locking between Kuramoto oscillators: Robustness to time-varying natural frequencies. In *IEEE Conf. on Decision and Control*, pages 1587–1592, Atlanta, USA, December 2010. doi:10.1109/CDC.2010.5717876.
- [13] L. Hörmander. *An Introduction to Complex Analysis in Several Variables*, volume 7 of *North-Holland Mathematical Library*. North-Holland Publishing Co, third edition, 1990.
- [14] A. Jadbabaie, N. Motee, and M. Barahona. On the stability of the Kuramoto model of coupled nonlinear oscillators. In *American Control Conference*, pages 4296–4301, Boston, USA, June 2004. doi:10.23919/ACC.2004.1383983.
- [15] S. Jafarpour and F. Bullo. Synchronization of Kuramoto oscillators via cutset projections. *IEEE Transactions on Automatic Control*, November 2017. Submitted. URL: <https://arxiv.org/abs/1711.03711>.
- [16] G. Jongen, J. Anemüller, D. Bollé, A. C. C. Coolen, and C. Perez-Vicente. Coupled dynamics of fast spins and slow exchange interactions in the XY spin glass. *Journal of Physics A: Mathematical and General*, 34(19):3957–3984, 2001. doi:10.1088/0305-4470/34/19/302.

- [17] I. Z. Kiss, Y. Zhai, and J. L. Hudson. Emerging coherence in a population of chemical oscillators. *Science*, 296(5573):1676–1678, 2002. doi:10.1126/science.1070757.
- [18] D. J. Klein, P. Lee, K. A. Morgansen, and T. Javidi. Integration of communication and control using discrete time Kuramoto models for multivehicle coordination over broadcast networks. *IEEE Journal on Selected Areas in Communications*, 26(4):695–705, 2008. doi:10.1109/JSAC.2008.080511.
- [19] J. Lavaei and S. H. Low. Zero duality gap in optimal power flow problem. *IEEE Transactions on Power Systems*, 27(1):92–107, 2012. doi:10.1109/TPWRS.2011.2160974.
- [20] J. M. Lee. *Introduction to Smooth Manifolds*. Springer, 2003.
- [21] D. C. Michaels, E. P. Matyas, and J. Jalife. Mechanisms of sinoatrial pacemaker synchronization: A new hypothesis. *Circulation Research*, 61(5):704–714, 1987. doi:10.1161/01.RES.61.5.704.
- [22] R. E. Mirollo and S. H. Strogatz. The spectrum of the locked state for the Kuramoto model of coupled oscillators. *Physica D: Nonlinear Phenomena*, 205(1-4):249–266, 2005. doi:10.1016/j.physd.2005.01.017.
- [23] J. Pantaleone. Stability of incoherence in an isotropic gas of oscillating neutrinos. *Physical Review D*, 58(7):073002, 1998. doi:10.1103/PhysRevD.58.073002.
- [24] V. Rakočević. On continuity of the Moore-Penrose and Drazin inverses. *Matematički Vesnik*, 49(3-4):163–172, 1997. URL: <http://www.emis.de/journals/MV/9734>.
- [25] R. Sepulchre, D. A. Paley, and N. E. Leonard. Stabilization of planar collective motion: All-to-all communication. *IEEE Transactions on Automatic Control*, 52(5):811–824, 2007. doi:10.1109/TAC.2007.898077.
- [26] J. W. Simpson-Porco, F. Dörfler, and F. Bullo. Synchronization and power sharing for droop-controlled inverters in islanded microgrids. *Automatica*, 49(9):2603–2611, 2013. doi:10.1016/j.automatica.2013.05.018.
- [27] P. A. Tass. A model of desynchronizing deep brain stimulation with a demand-controlled coordinated reset of neural subpopulations. *Biological Cybernetics*, 89(2):81–88, 2003. doi:10.1007/s00422-003-0425-7.
- [28] M. Verwoerd and O. Mason. Global phase-locking in finite populations of phase-coupled oscillators. *SIAM Journal on Applied Dynamical Systems*, 7(1):134–160, 2008. doi:10.1137/070686858.
- [29] M. Verwoerd and O. Mason. On computing the critical coupling coefficient for the Kuramoto model on a complete bipartite graph. *SIAM Journal on Applied Dynamical Systems*, 8(1):417–453, 2009. doi:10.1137/080725726.
- [30] F. Wu and S. Kumagai. Steady-state security regions of power systems. *IEEE Transactions on Circuits and Systems*, 29(11):703–711, 1982. doi:10.1109/TCS.1982.1085091.
- [31] R. D. Zimmerman, C. E. Murillo-Sánchez, and R. J. Thomas. MATPOWER: Steady-state operations, planning, and analysis tools for power systems research and education. *IEEE Transactions on Power Systems*, 26(1):12–19, 2011. doi:10.1109/TPWRS.2010.2051168.